AIAA JOURNAL
Vol. 41, No. 11, November 2003

Exact Solutions of Cross-Ply Laminates with Bonding Imperfections

W. Q. Chen,* J. B. Cai,† and G. R. Ye†
Zhejiang University, 310027 Hangzhou, People's Republic of China

State-space approach is developed to analyze the bending and free vibration of a simply supported, cross-ply laminated rectangular plate featuring interlaminar bonding imperfections, for which a general linear spring layer model is adopted. The analysis is directly based on the three-dimensional theory of orthotropic elasticity and is completely exact. Numerical comparison is made, showing that although the plate theory developed in the literature behaves well for moderately thick perfect laminates it can become inaccurate when bonding imperfections are present. The special problem of the laminate in cylindrical bending is also considered, and the validity of the assumption of cylindrical bending is investigated through numerical examples.

Nomenclature

$\boldsymbol{A}$	=	dimensionless coefficient matrix
a, b, h	=	length, width and height of plate
c_{ij}	=	elastic constants
E, G, μ	=	Young's modulus, shear modulus, and Poisson's ratio
h_k	=	thickness of the kth layer
K_i	=	stiffness constants of interface
$\boldsymbol{M}_k, \boldsymbol{P}_k$	=	transfer matrices of layer and interface
m, n	=	positive integers
N	=	number of layers in the laminate
$\boldsymbol{T}, T_{ij}$	=	global transfer matrix and the elements
u, v, w	=	displacement components in Cartesian coordinates
$\boldsymbol{V}$	=	dimensionless state vector
z_k	=	z coordinate of the kth interface
ξ, η, ζ	=	dimensionless coordinates
ρ	=	mass density ratio
σ_i, τ_{ij}	=	normal and shear-stress components
$\Omega, \omega^0, \omega^*$	=	dimensionless frequency parameters
ω	=	circular frequency

Subscripts

L, T	=	directions parallel and perpendicular to the fibers
k	=	kth layer or interface

Superscript

(k)	=	kth layer

Introduction

IN the traditional theory of structural analysis of composites, any two adjacent layers in a laminate are usually assumed to be bonded perfectly.[1] However, various flaws, such as microcracks, inhomogeneities, and cavities, can be introduced into the bond in the process of fabrication. During the service lifetime, the structure will be subjected to various (dynamic, cyclic, or long term) loads and exposed to corrosive environment. Consequently, these tiny flaws can get significant and finally lead to the local failure of bond or even the whole collapse of structure. Thus it is very important to study the effect of bond imperfections on behavior of laminated structures. The thermoelastic fields in orthotropic layered slabs or cylinders with imperfect interfaces were studied by Blandford and Tauchert[2] by a finite element technique. Somers et al.[3] developed an analytical beam model of sandwich beams containing lengthwise and depthwise through-the-width delaminations; the effect of delaminations on the buckling and postbuckling of the beam was investigated. Cheng et al.[4–6] first introduced the spring-layer model[7,8] to describe the weakness of interlaminar bonding into structural analyses of laminated plates and shells. Di Sciuva[9] derived the controlling equations for laminated plates with interlaminar slips involving geometric nonlinearity. Icardi[10] presented a free-vibration analysis of composite beams with imperfect bonding. Icardi et al.[11] further considered the effect of interlaminar bonding imperfection on the behavior of adaptive beam structures. More recently, Librescu and Schmidt[12] developed a general linear theory of laminated composite anisotropic shells featuring interlaminar bonding imperfections; a research survey on the subject can also be found there.

There are a lot of three-dimensional exact solutions available in literature for perfectly bonded laminated plates and shells.[13–17] These solutions have played an important role in clarifying simplified two-dimensional plate and shell theories or numerical methods. However, no similar work on laminates with imperfect bonding can be found yet. It is the aim of this study to present such an exact analysis of simply supported cross-ply laminates featuring interlaminar bonding imperfections.

The generalization of available exact solutions for laminates with imperfect bonding will not involve extra mathematical difficulty, provided that the spring-layer model is employed. For example, in the famous Pagano's solution for cylindrical bending[13] the expressions for two nonzero displacements are still valid in each layer. By replacing the continuity conditions of displacements with the interfacial Hooke's relations between the displacements and stresses for the spring-layer model, a set of linear algebraic equations about the undetermined integral constants can be similarly obtained. In this paper, however, we will not follow such an analysis because it seems computationally expensive when the laminate is made up of a large number of plies. For instance, there will be totally $4N$ undermined constants in Pagano's solution[13] for a N-layered cross-ply laminate in cylindrical bending.

Instead, we will employ here the state-space approach to analyze the bending and free vibration of cross-ply laminates with imperfect bonding. In this method the final solving equations remain the same scale no matter how many layers are involved in the laminate. The state-space approach has been developed and employed widely to analyze traditional perfect laminates and proved to be very powerful.[18–23] This seems, however, to be the first time to exploit its application in structural analysis of imperfectly bonded laminates.

Received 30 April 2003; revision received 1 July 2003; accepted for publication 2 July 2003.

*Professor, Department of Civil Engineering; chenwq@ccea.zju.edu.cn.
†Associate Professor, Department of Civil Engineering.

Compared to the analysis of perfect laminates, only a special but direct treatment of the conditions at interfaces (spring-layer model) is necessary. This results in a so-called interfacial transfer matrix, which will degenerate to the unit matrix for a perfect laminate. Numerical results for bending and free vibration of various laminates with uniform or nonuniform interlaminar imperfection in shear are presented. The state equation for the problem of laminates in cylindrical bending is also presented. A detailed numerical investigation is made to clarify the validity of the assumption of cylindrical bending for a rectangular laminate.

State-Space Formulations

We consider a N-layered cross-ply rectangular laminate as shown in Fig. 1. The constitutive relations read as[1]

$$\sigma_x = c_{11}\frac{\partial u}{\partial x} + c_{12}\frac{\partial v}{\partial y} + c_{13}\frac{\partial w}{\partial z}, \qquad \sigma_y = c_{12}\frac{\partial u}{\partial x} + c_{22}\frac{\partial v}{\partial y} + c_{23}\frac{\partial w}{\partial z}$$

$$\sigma_z = c_{13}\frac{\partial u}{\partial x} + c_{23}\frac{\partial v}{\partial y} + c_{33}\frac{\partial w}{\partial z}, \qquad \tau_{yz} = c_{44}\left(\frac{\partial v}{\partial z} + \frac{\partial w}{\partial y}\right)$$

$$\tau_{xz} = c_{55}\left(\frac{\partial u}{\partial z} + \frac{\partial w}{\partial x}\right), \qquad \tau_{xy} = c_{66}\left(\frac{\partial u}{\partial y} + \frac{\partial v}{\partial x}\right) \tag{1}$$

Fan and Ye[19] derived the following state equation from Eq. (1) and the equations of motion:

$$\frac{\partial}{\partial z}\begin{Bmatrix}\sigma_z\\ u\\ v\\ w\\ \tau_{xz}\\ \tau_{yz}\end{Bmatrix} = \begin{bmatrix} \mathbf{0} & \begin{matrix} \rho\frac{\partial^2}{\partial t^2} & -\frac{\partial}{\partial x} & -\frac{\partial}{\partial y} \\ & \frac{1}{c_{55}} & 0 \\ \text{sym.} & & \frac{1}{c_{44}} \end{matrix} \\ \begin{matrix} \frac{1}{c_{33}} & -\frac{c_{13}}{c_{33}}\frac{\partial}{\partial x} & -\frac{c_{23}}{c_{33}}\frac{\partial}{\partial y} \\ & \rho\frac{\partial^2}{\partial t^2} - \beta_1\frac{\partial^2}{\partial x^2} - c_{66}\frac{\partial^2}{\partial y^2} & -\beta_2\frac{\partial^2}{\partial x\partial y} \\ \text{sym.} & & \rho\frac{\partial^2}{\partial t^2} - \beta_3\frac{\partial^2}{\partial y^2} - c_{66}\frac{\partial^2}{\partial x^2} \end{matrix} & \mathbf{0} \end{bmatrix}\begin{Bmatrix}\sigma_z\\ u\\ v\\ w\\ \tau_{xz}\\ \tau_{yz}\end{Bmatrix} \tag{2}$$

where σ_z, u, v, w, τ_{xz}, and τ_{yz} are termed as state variables, from which the three induced variables can be determined as

$$\sigma_x = \frac{c_{13}}{c_{33}}\sigma_z + \beta_1\frac{\partial u}{\partial x} + \beta_4\frac{\partial v}{\partial y}$$

$$\sigma_y = \frac{c_{23}}{c_{33}}\sigma_z + \beta_4\frac{\partial u}{\partial x} + \beta_3\frac{\partial v}{\partial y}, \qquad \tau_{xy} = c_{66}\left(\frac{\partial u}{\partial y} + \frac{\partial v}{\partial x}\right) \tag{3}$$

where

$$\beta_1 = c_{11} - c_{13}^2/c_{33}, \qquad \beta_2 = c_{12} + c_{66} - c_{13}c_{23}/c_{33}$$

$$\beta_3 = c_{22} - c_{23}^2/c_{33}, \qquad \beta_4 = \beta_2 - c_{66} \tag{4}$$

An exact solution can be obtained for the simply supported boundary conditions by assuming[19]

$$\begin{Bmatrix}\sigma_z\\ u\\ v\\ w\\ \tau_{xz}\\ \tau_{yz}\end{Bmatrix} = \begin{Bmatrix} -c_{44}^{(1)}\bar{\sigma}_z(\zeta)\sin(m\pi\xi)\sin(n\pi\eta)\\ h\bar{u}(\zeta)\cos(m\pi\xi)\sin(n\pi\eta)\\ h\bar{v}(\zeta)\sin(m\pi\xi)\cos(n\pi\eta)\\ h\bar{w}(\zeta)\sin(m\pi\xi)\sin(n\pi\eta)\\ c_{44}^{(1)}\bar{\tau}_{xz}(\zeta)\cos(m\pi\xi)\sin(n\pi\eta)\\ c_{44}^{(1)}\bar{\tau}_{yz}(\zeta)\sin(m\pi\xi)\cos(n\pi\eta)\end{Bmatrix}\exp(i\omega t) \tag{5}$$

where $\xi = x/a$, $\eta = y/b$, and $\zeta = z/h$, and m and n are the half-wave numbers in x and y directions, respectively. The substitution of Eq. (5) into Eq. (2) yields

$$\frac{\mathrm{d}}{\mathrm{d}\zeta}\boldsymbol{V}(\zeta) = \boldsymbol{A}\boldsymbol{V}(\zeta) \tag{6}$$

where $\boldsymbol{V}(\zeta) = [\bar{\sigma}_z(\zeta), \bar{u}(\zeta), \bar{v}(\zeta), \bar{w}(\zeta), \bar{\tau}_{xz}(\zeta), \bar{\tau}_{yz}(\zeta)]^T$ and

$$\boldsymbol{A} = \begin{bmatrix} \mathbf{0} & \begin{matrix} \frac{\rho}{\rho^{(1)}}\Omega^2 & -t_1 & -t_2 \\ & \frac{c_{44}^{(1)}}{c_{55}} & 0 \\ \text{sym.} & & \frac{c_{44}^{(1)}}{c_{44}} \end{matrix} \\ \begin{matrix} -\frac{c_{44}^{(1)}}{c_{33}} & \frac{c_{13}}{c_{33}}t_1 & \frac{c_{23}}{c_{33}}t_2 \\ & -\frac{\rho}{\rho^{(1)}}\Omega^2 + \frac{\beta_1}{c_{44}^{(1)}}t_1^2 + \frac{c_{66}}{c_{44}^{(1)}}t_2^2 & \frac{\beta_2}{c_{44}^{(1)}}t_1t_2 \\ \text{sym.} & & -\frac{\rho}{\rho^{(1)}}\Omega^2 + \frac{\beta_3}{c_{44}^{(1)}}t_2^2 + \frac{c_{66}}{c_{44}^{(1)}}t_1^2 \end{matrix} & \mathbf{0} \end{bmatrix} \tag{7}$$

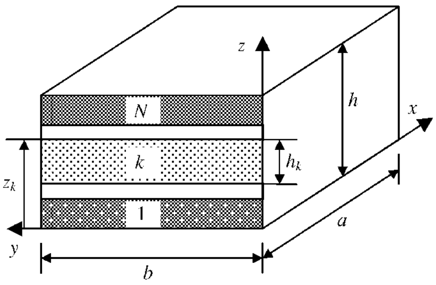

Fig. 1 Geometry and coordinates of rectangular laminate.

with $t_1 = m\pi h/a$, $t_2 = n\pi h/b$, and $\Omega = \omega h\sqrt{(\rho^{(1)}/c_{44}^{(1)})}$. The solution to Eq. (6) can be obtained as

$$V(\zeta) = e^{A(\zeta - \zeta_{k-1})} V(\zeta_{k-1})$$
$$(\zeta_{k-1} \le \zeta \le \zeta_k, \qquad k = 1, 2, \ldots, N) \tag{8}$$

where $\zeta_0 = 0$ and $\zeta_k = z_k/h$. Setting $\zeta = \zeta_k$ in Eq. (8) yields

$$V_1^{(k)} = M_k V_0^{(k)} \tag{9}$$

where $V_1^{(k)}$ and $V_0^{(k)}$ are the state vectors at the upper and lower surfaces and $M_k = e^{A(\zeta_k - \zeta_{k-1})}$. Similarly, we get

$$V_1^{(k+1)} = M_{k+1} V_0^{(k+1)} \tag{10}$$

Imperfect Bonding Conditions

A general spring-layer model is adopted here to describe the imperfect bonding[4–6,12]:

$$\sigma_z^{(k+1)} = \sigma_z^{(k)} = K_z^{(k)}\left[w^{(k+1)} - w^{(k)}\right]$$
$$\tau_{xz}^{(k+1)} = \tau_{xz}^{(k)} = K_x^{(k)}\left[u^{(k+1)} - u^{(k)}\right]$$
$$\tau_{yz}^{(k+1)} = \tau_{yz}^{(k)} = K_y^{(k)}\left[v^{(k+1)} - v^{(k)}\right] \qquad \text{at} \qquad z = z_k \tag{11}$$

It is clear that when the bonding stiffness constants $K_i^{(k)} \to \infty$ the displacements will be continuous across the interface, implying a perfect bonding, whereas $K_i^{(k)} = 0$ indicates that the kth layer and $(k+1)$th layer are completely separated from each other.

Noticing Eq. (5), Eq. (11) can be expressed as follows:

$$V_0^{(k+1)} = P_k V_1^{(k)} \tag{12}$$

where

$$P_k = \begin{bmatrix} 1 & 0 & 0 & 0 & 0 & 0 \\ 0 & 1 & 0 & 0 & R_x^{(k)} & 0 \\ 0 & 0 & 1 & 0 & 0 & R_y^{(k)} \\ -R_z^{(k)} & 0 & 0 & 1 & 0 & 0 \\ 0 & 0 & 0 & 0 & 1 & 0 \\ 0 & 0 & 0 & 0 & 0 & 1 \end{bmatrix} \tag{13}$$

with $R_i^{(k)} = c_{44}^{(1)}/[K_i^{(k)} h]$ $(i = x, y, z)$ being dimensionless compliance coefficients of the interfaces, which vanish for a perfect interface.

From Eqs. (9), (10), and (12) a relation between state vectors at the upper surface of the $(k+1)$th layer and the lower surface of the kth layer is established

$$V_1^{(k+1)} = M_{k+1} P_k M_k V_0^{(k)} \tag{14}$$

Continuing the preceding procedure, the relation between state vectors at the top and bottom surfaces of the laminate is finally obtained as

$$V_1^{(N)} = T V_0^{(1)} \tag{15}$$

where

$$T = \left(\prod_{j=N}^{2} M_j P_{j-1}\right) M_1$$

In the case of a perfectly bonded laminate, all P_j become unit matrix, yielding

$$T = \prod_{j=N}^{1} M_j$$

which is exactly the same as that derived by Fan and Ye.[19]

Bending and Free-Vibration Analysis

Because Eq. (15) has the same structure as that for a perfect laminate,[19] details of bending and free-vibration analysis are omitted here for brevity. We only give the final solving equation in the following. When the laminate is traction-free at the top and bottom surfaces, we can get the frequency equation from Eq. (15) as

$$\begin{vmatrix} T_{12} & T_{13} & T_{14} \\ T_{52} & T_{53} & T_{54} \\ T_{62} & T_{63} & T_{64} \end{vmatrix} = 0 \tag{16}$$

After the frequency ω is solved from Eq. (16), the vibrational modes of displacements at the bottom surface can be obtained from Eq. (15). The state vector for any value of ζ can then be determined by

$$V(\zeta) = e^{A(\zeta - \zeta_0)} V_0^{(1)}, \qquad (\zeta_0 \le \zeta \le \zeta_1)$$
$$V(\zeta) = e^{A(\zeta - \zeta_1)} P_1 M_1 V_0^{(1)}, \qquad (\zeta_1 \le \zeta \le \zeta_2)$$
$$V(\zeta) = e^{A(\zeta - \zeta_{k-1})}\left(\prod_{j=k-1}^{2} M_j P_{j-1}\right) M_1 V_0^{(1)}$$
$$(\zeta_{k-1} \le \zeta \le \zeta_k, \qquad k = 3, 4, \ldots, N) \tag{17}$$

The three induced variables are calculated from the state variables by Eq. (3).

For bending problem ($\omega = 0$), if generally distributed normal pressures $p(x, y)$ and $q(x, y)$ are applied on the bottom and top surfaces, respectively, we can expand the loads in terms of double sine functions as follows:

$$p(x, y) = c_{44}^{(1)} \sum_{m=1}^{\infty}\sum_{n=1}^{\infty} a_{mn} \sin(m\pi\xi)\sin(n\pi\eta)$$
$$q(x, y) = c_{44}^{(1)} \sum_{m=1}^{\infty}\sum_{n=1}^{\infty} b_{mn} \sin(m\pi\xi)\sin(n\pi\eta) \tag{18}$$

where

$$[a_{mn}, b_{mn}] = \left[\frac{4}{c_{44}^{(1)}}\right] \int_0^1\int_0^1 [p(\xi, \eta), q(\xi, \eta)] \times \sin(m\pi\xi)\sin(n\pi\eta)\, d\xi\, d\eta$$

Then, for an arbitrary couple of (m, n) we have

$$\begin{Bmatrix} \bar{u}(0) \\ \bar{v}(0) \\ \bar{w}(0) \end{Bmatrix} = \begin{bmatrix} T_{12} & T_{13} & T_{14} \\ T_{52} & T_{53} & T_{54} \\ T_{62} & T_{63} & T_{64} \end{bmatrix}^{-1} \begin{Bmatrix} b_{mn} - T_{11}a_{mn} \\ -T_{51}a_{mn} \\ -T_{61}a_{mn} \end{Bmatrix} \tag{19}$$

The state vector for an arbitrary value of ζ and the induced variables are still determined from Eqs. (17) and (3), respectively.

For a cross-ply laminate with $b \to \infty$, the so-called cylindrical bending problem arises.[13] In this case we have only two nonzero displacements u and w, in x and z directions, respectively, and both are independent of the coordinate y. The corresponding state equations can be obtained as

$$\frac{\partial}{\partial z}\begin{Bmatrix}\sigma_z\\ u\\ w\\ \tau_{xz}\end{Bmatrix}=\begin{bmatrix}0 & 0 & \rho\dfrac{\partial^2}{\partial t^2} & -\dfrac{\partial}{\partial x}\\ 0 & 0 & -\dfrac{\partial}{\partial x} & \dfrac{1}{c_{55}}\\ \dfrac{1}{c_{33}} & -\dfrac{c_{13}}{c_{33}}\dfrac{\partial}{\partial x} & 0 & 0\\ -\dfrac{c_{13}}{c_{33}}\dfrac{\partial}{\partial x} & \rho\dfrac{\partial^2}{\partial t^2}-\beta_1\dfrac{\partial^2}{\partial x^2} & 0 & 0\end{bmatrix}\begin{Bmatrix}\sigma_z\\ u\\ w\\ \tau_{xz}\end{Bmatrix} \tag{20}$$

The proceeding analysis is then similar and omitted here for brevity.

Numerical Examples

For all cases to be considered, the stacking sequence of laminate is always from the top ($\zeta = 1$) to bottom ($\zeta = 0$), and the notation system in Whitney[1] is adopted. Each layer involved in the N-layered laminate is considered to have the same thickness (h/N) and density. As regards the imperfections of interfacial bonding, we always take $R_z^{(k)} = 0$ to avoid the possibility of material penetration phenomenon that is physically impossible.[4–6] In this case any two adjacent layers contact with each other to ensure the continuity of transverse displacement w, but allow a shear sliding in the plate plane. We also assume the two compliance constants in the plate surface are the same, and a dimensionless parameter $E_T/[K_x^{(k)}h] = E_T/[K_y^{(k)}h] = R^{(k)}$ is adopted hereafter.

In the following, if bending problem is considered, we always assume that a normal sinusoidal pressure $q = q_0 \sin(\pi\xi)\sin(\pi\eta)$ is applied at the top surface of the laminate. In addition, if it is not clear with which layer a physical quantity at an interface is associated the quantity is usually followed by a superscript indicating the sequence number of the layer, just as that done earlier in this paper; otherwise, the superscript will be omitted for brevity.

It seems unnecessary to validate the present method because the derivation here is a straightforward generalization of that presented in Ref. 19. However, numerical comparison with existent results can demonstrate the correctness of program and can help one to get a deep insight into the available results. Table 1 compares the results of our method with those of the plate theory (data in parentheses)[4] for a four-layered square laminate with layerup sequence [0/90/90/0 deg]. In Table 1 results predicted by the exact three-dimensional solution of Pagano and Hatfield[14] for the perfect laminate are also given in square brackets, which are cited directly from Ref. 4. The following typical material properties are employed:

$$E_L/E_T = 25, \qquad G_{LT}/E_T = 0.5$$
$$G_{TT}/E_T = 0.2, \qquad \mu_{LT} = \mu_{TT} = 0.25 \tag{21}$$

A uniform imperfect bond is assumed in this example, that is, $R^{(k)} = R$. It is shown that, as expected, the present exact solution is almost identical to the Pagano and Hatfield's exact solution, except the central deflection of the laminate with a relative error only about 1% for all three values of a/h. The difference of w might be caused by different computational precision. As we know, the plate theory predication should approach the exact three-dimensional one in the case of a very thin perfect plate. This is demonstrated in Table 1 for $a/h = 100$ by comparing our results with that of the plate theory. The two are almost identical when $R = 0$. From this point of view, our results of deflection should be more exact. Table 1 also shows that although the plate theory[4] can give a satisfactory prediction for thick perfect laminate the presence of interfacial flaw can make its accuracy worse, especially for large R. In particular, the deflection obtained by the plate theory is generally larger than that by the present three-dimensional solution for imperfect laminates. Thus, if engineer wants to control the deflection of an imperfect laminate structure based on the results of plate theory a conservative design can be obtained. On the other hand, if he wants to determine the degree of interfacial damage of a practical structure in service by comparing the experimental results of deflection with the plate theory's prediction he might underestimate the deteriorate. It is also worth pointing out that because the plate theory underestimates the

Table 1 Simply supported square laminate ([0/90/90/0 deg]) with uniform interfacial imperfection under sinusoidal load[a,b]

a/h	R	w_0	σ_1	$\sigma_2^{(3)}$	τ_{12}	τ_{13}	τ_{23}
4	0	−1.93672	−0.72026	−0.66255	−0.04581	−0.21933	−0.29152
		[−1.954]	[−0.720]	[−0.663]	[−0.0458]	[−0.219]	[−0.292]
		(−1.90601)	(−0.73681)	(−0.70013)	(−0.04343)	(−0.21093)	(−0.31484)
	0.2	−2.21171	−0.78585	−0.70719	−0.04988	−0.21051	−0.26391
		(−2.48111)	(−0.88504)	(−0.77606)	(−0.04940)	(−0.19365)	(−0.28178)
	0.4	−2.45815	−0.84389	−0.75108	−0.05340	−0.20179	−0.24274
		(−3.08282)	(−1.04440)	(−0.86434)	(−0.05590)	(−0.17620)	(−0.23683)
	0.6	−2.68113	−0.89607	−0.79326	−0.05648	−0.19348	−0.22568
		(−3.66623)	(−1.20036)	(−0.96086)	(−0.06253)	(−0.15819)	(−0.18941)
10	0	−0.73698	−0.55861	−0.40096	−0.02764	−0.30137	−0.19595
		[−0.743]	[−0.559]	[−0.401]	[−0.0276]	[−0.301]	[−0.196]
		(−0.73590)	(−0.56107)	(−0.40806)	(−0.02735)	(−0.30017)	(−0.19954)
	0.2	−0.79688	−0.56983	−0.42079	−0.02885	−0.29592	−0.19876
		(−0.86150)	(−0.58204)	(−0.44976)	(−0.02943)	(−0.28870)	(−0.21079)
	0.4	−0.85492	−0.58106	−0.43948	−0.03001	−0.29104	−0.19582
		(−1.00458)	(−0.60938)	(−0.49188)	(−0.03163)	(−0.27757)	(−0.21804)
	0.6	−0.91203	−0.59224	−0.45716	−0.03112	−0.28606	−0.20251
		(−1.16323)	(−0.64260)	(−0.53417)	(−0.03394)	(−0.26688)	(−0.22125)
100	0	−0.43460	−0.53885	−0.27101	−0.02136	−0.33880	−0.13894
		[−0.4385]	[−0.539]	[−0.271]	[−0.0214]	[−0.339]	[−0.139]
		(−0.43460)	(−0.53887)	(−0.27106)	(−0.02135)	(−0.33879)	(−0.13897)
	0.2	−0.43530	−0.53894	−0.27134	−0.02137	−0.33871	−0.13905
		(−0.43611)	(−0.53903)	(−0.27178)	(−0.02139)	(−0.33859)	(−0.13924)
	0.4	−0.43601	−0.53904	−0.27166	−0.02139	−0.33861	−0.13915
		(−0.43789)	(−0.53923)	(−0.27261)	(−0.02142)	(−0.33836)	(−0.13955)
	0.6	−0.43671	−0.53913	−0.27199	−0.02140	−0.33852	−0.13926
		(−0.43995)	(−0.53948)	(−0.27356)	(−0.02146)	(−0.33810)	(−0.13988)

[a]Data in square brackets are calculated by three-dimensional solution,[14] and those in parentheses are obtained by plate theory.[4] All of these data are directly cited from Table 2 of Ref. 4.

[b]$w_0 = 100E_T h^3 w(a/2, b/2, h/2)/(q_0 a^4)$, $\sigma_1 = h^2\sigma_x(a/2, b/2, h)/(q_0 a^2)$, $\sigma_2 = h^2\sigma_y(a/2, b/2, 3h/4)/(q_0 a^2)$, $\tau_{12} = h^2\tau_{xy}(0, 0, 0)/(q_0 a^2)$, $\tau_{13} = h\tau_{xz}(0, b/2, h/2)/(q_0 a)$, $\tau_{23} = h\tau_{yz}(a/2, 0, h/2)/(q_0 a)$.

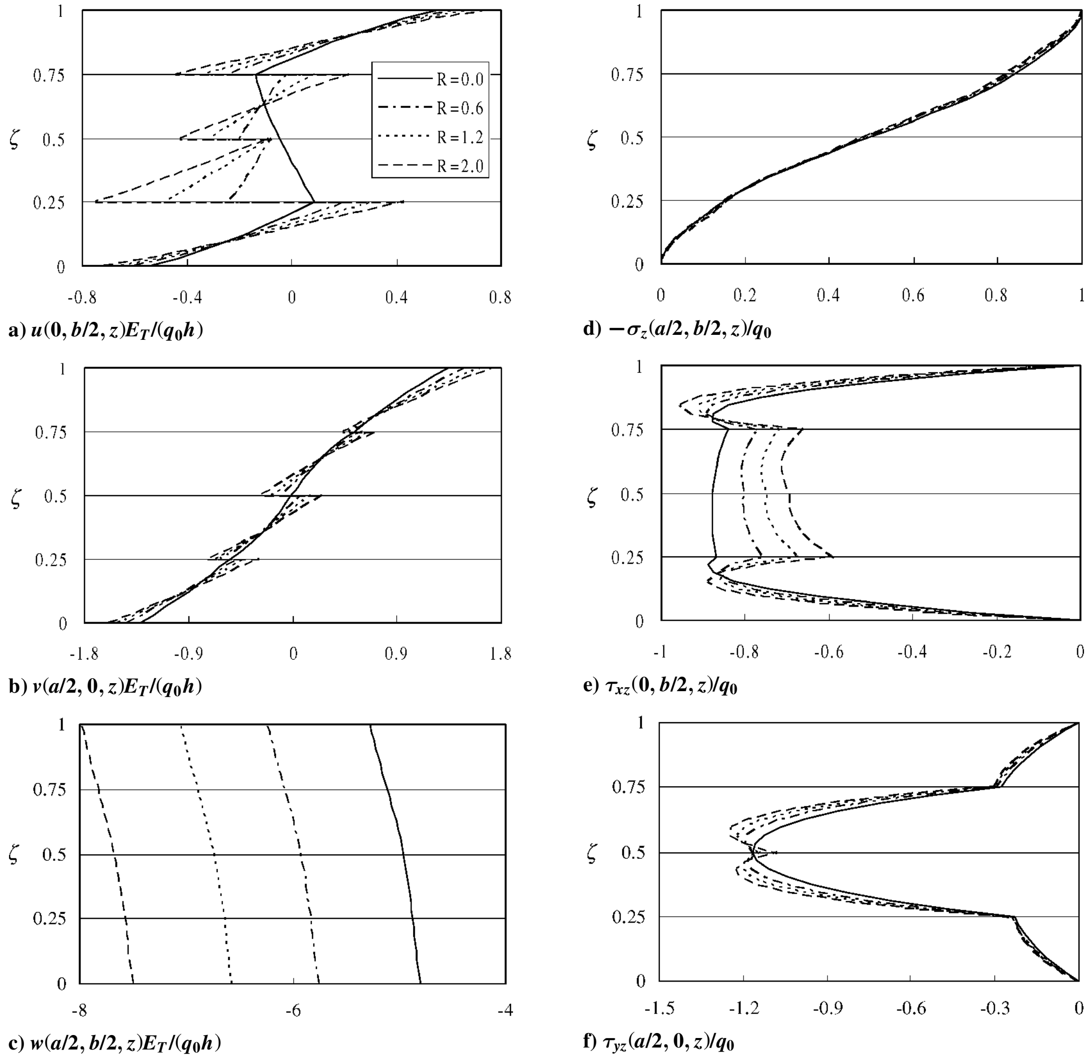

Fig. 2 Distributions of normalized state variables along the thickness direction.

transverse shear stresses for several cases, as shown in Table 1, the use of such an approximate theory to predict the interfacial strength should be very careful in engineering. To sum up, it is very important to develop accurate analysis method for laminates with bonding imperfections.

The distributions along the thickness direction of stresses and displacements are given in Fig. 2 for the preceding square laminate of $a/h = b/h = 4$, but with nonuniform imperfections $[R^{(1)} = 4R^{(2)} = 2R^{(3)} = R]$. As expected, the tangential displacements u and v are discontinuous across the three interfaces for $R \neq 0$ because of the imperfections. As we know, weak interfaces can be knowingly introduced into a laminate to increase its interfacial fracture toughness.[24] This is partly demonstrated in Figs. 2e and 2f. By selecting a proper distribution of bonding imperfection, it can be expected that the transverse stress τ_{yz} at the second interface can be reduced more significantly. Moreover, because the deflection increases with R, that is, the rigidity of the laminate decreases, one should seek an optimum value of R for improving the interfacial fracture toughness as well as keeping the structural rigidity to satisfy the practical requirement. The optimization of bonding imperfections is a very challenging topic requiring further investigations, which is out of the scope of this paper.

As mentioned in the last section, when the laminate has one side much longer than the other one can solve the problem under the assumption of cylindrical bending, for which the state equation is shown in Eq. (20). Table 2 lists the normalized displacement $-100E_Th^3w/(q_0a^4)$ at the point $(a/2, b/2, h/2)$ of a rectangular laminate for several cases. We still employ the material constants given in Eq. (21) and assume a uniform imperfection. The results for $b/h \to \infty$ are calculated directly based on the formulations for cylindrical bending problem.

It can be seen that, for the perfect laminate, our results for cylindrical bending are identical to those of Pagano's exact solution,[13] which are directly cited from Table 1 in Ref. 25. Table 2 shows that when b/a of the rectangular laminate increases the results converge rapidly to that of the cylindrical bending problem. The cylindrical bending solution appears to be the upper limit of that of the rectangular laminate. That is true because it can be regarded that the constraints at $y = 0, b$ are released when the laminate is in the state of cylindrical bending, leading to a relatively large deflection. It can be found that the relative errors between the rectangular laminate with $b/a = 5$ and the laminate in cylindrical bending are less than 1.5% for all parameters. This indicates that when $b/a > 5$ one can use the equations for cylindrical bending, which are much simpler than the original equations, to give an initial analysis for the purpose of engineering design. Of course, the relative error varies with various parameters. It is smaller for the three-ply laminate than for the seven-ply one, and it will become a little large if the laminate is thick. Also, it increases with the interfacial compliance coefficient R. Thus, a further exact analysis is also needed to assure the correctness of the initial one.

Considering the free-vibration problem, we take the following material constants[16] for comparison purpose:

$$E_L = 25.1, \qquad E_T = 4.8, \qquad E_z = 0.75$$
$$G_{LT} = 1.36, \qquad G_{Lz} = 1.2, \qquad G_{Tz} = 0.47$$
$$\mu_{LT} = 0.036, \qquad \mu_{Lz} = 0.25, \qquad \mu_{Tz} = 0.171 \quad (22)$$

The first 10 lowest frequency parameters $\omega^0 = \omega h\sqrt{(\rho/E_T)}$ are given in Table 3 for a simply supported square laminate of $a/h = b/h = 10$ and with stacking sequence [0/90/0/90 deg]. Nonuniform imperfections are assumed, that is, $R^{(1)} = 4R^{(2)} = 2R^{(3)} = R$. For a perfect laminate results are found to be identical to those predicted by the exact three-dimensional solution,[15] which are directly cited from Table 6 in Ref. 26. It is shown that with the increase of R the frequency of the laminate decreases because of the reduction of stiffness. We also list in Table 3 the relative error between the perfect laminate and the imperfect one with $R = 1.0$. From the results it is seen that the sensitivity of frequency to the interfacial damage obviously depends on the frequency order. For example when $m = n = 1$, the relative error for the first lowest natural frequency is 2.70%, whereas it becomes 15.21% for the seventh frequency. Knowing such a difference is useful in nondestructive inspection of damaged structures employing dynamic technologies. It is especially very important for the reliable and precise evaluation of structural damage to stimulate proper vibrational modes, of which the frequencies vary significantly with the interfacial flaws.

Table 2 Normalized center deflection $-100E_T h^3 w(a/2, b/2, h/2)/(q_0 a^4)$ of a simply supported rectangular laminate with uniform interfacial imperfection[a]

Stacking sequence	a/h	b/h	$R = 0$	$R = 0.2$	$R = 0.4$	$R = 0.6$
[0/90/0 deg]	4	4	2.00591	2.17442	2.32199	2.45278
		20	2.86585	3.17051	3.44407	3.69109
		50	2.88400	3.19182	3.46840	3.71828
		100	2.88643	3.19466	3.47164	3.72189
		200	2.88703	3.19536	3.47244	3.72279
		∞	2.88723 (2.8872)	3.19560	3.47271	3.72309
	10	10	0.753030	0.803016	0.850977	0.897048
		50	0.927368	0.997540	1.06604	1.13293
		100	0.930608	1.00111	1.06994	1.13716
		200	0.931386	1.00196	1.07087	1.13817
		300	0.931529	1.00212	1.07104	1.13836
		∞	0.931643 (0.93164)	1.00224	1.07118	1.13851
[(0/90)$_3$0 deg]	4	4	1.81048	2.32660	2.81370	3.27469
		20	3.07962	3.99021	4.85704	5.68390
		50	3.10684	4.03008	4.91033	5.75096
		100	3.10999	4.03468	4.91648	5.75876
		200	3.11074	4.03578	4.91796	5.76062
		∞	3.11099 (3.1110)	4.03614	4.91844	5.76124
	10	10	0.664809	0.757462	0.848775	0.938873
		50	1.07263	1.23163	1.38908	1.54504
		100	1.07820	1.23828	1.39688	1.55405
		200	1.07941	1.23971	1.39854	1.55595
		300	1.07946	1.23996	1.39883	1.55629
		∞	1.07980 (1.0798)	1.24016	1.39907	1.55655

[a]Data in parentheses calculated by Pagano's three-dimensional solution[13]; see Table 1 in Ref. 25.

Table 4 Lowest natural frequency parameter $\omega^* = \omega h\sqrt{(\rho/G_{LT})}$ of a simply supported rectangular laminate with uniform interfacial imperfection ($a/h = 10$, $m = n = 1$)[a]

Stacking sequence	b/h	$R = 0$	$R = 0.2$	$R = 0.4$	$R = 0.6$
[0/90 deg]	10	0.126184	0.125906	0.125633	0.125367
	50	0.0824861	0.0823791	0.0822737	0.0821700
	100	0.0818784	0.0817746	0.0816723	0.0815716
	200	0.0817399	0.0816368	0.0815352	0.0814353
	300	0.0817150	0.0816120	0.0815105	0.0814107
	∞	0.0816952 (0.0816952)	0.0815923	0.0814909	0.0813912
[0/90/0 deg]	10	0.162031	0.156948	0.152493	0.148552
	50	0.146560	0.141338	0.136742	0.132660
	100	0.146323	0.141104	0.136510	0.132429
	200	0.146267	0.141048	0.136455	0.132374
	300	0.146256	0.141038	0.136444	0.132364
	∞	0.146248 (0.146248)	0.141030	0.136436	0.132356
[0/90/0/90 deg]	10	0.160967	0.155299	0.150295	0.145838
	50	0.110085	0.106327	0.102997	0.100022
	100	0.109595	0.105838	0.102509	0.0995340
	200	0.109493	0.105736	0.102407	0.0994331
	300	0.109475	0.105718	0.102390	0.0994154
	∞	0.109461 (0.109461)	0.105704	0.102376	0.0994014
[(0/90)$_2$0 deg]	10	0.169802	0.161699	0.154786	0.148798
	50	0.140279	0.132986	0.126793	0.121451
	100	0.139978	0.132692	0.126503	0.121164
	200	0.139912	0.132627	0.126439	0.121102
	300	0.139900	0.132616	0.126428	0.121091
	∞	0.139891 (0.139891)	0.132606	0.126419	0.121082

[a]Data in parentheses calculated by alternative three-dimensional solution; see Table 1 in Ref. 27.

Table 3 Lowest 10 frequency parameters $\omega^0 = \omega h\sqrt{(\rho/E_T)}$ of a simply supported square laminate with nonuniform interfacial imperfections ($a/h = 10$, [0/90/0/90 deg])[a]

(m, n)	Order	$R = 0$	$R = 0.2$	$R = 0.5$	$R = 1.0$	R.E., %[b]
(1, 1)	1	0.0662101 (0.06621)	0.0658372	0.0652922	0.0644200	3.21
	2	0.545959 (0.54596)	0.545245	0.544179	0.542416	0.52
	3	0.599955 (0.59996)	0.599245	0.598173	0.596366	0.48
	4	1.24253 (1.2425)	1.24197	1.22890	1.17240	6.90
	5	1.29879 (1.2988)	1.27106	1.24481	1.20616	8.58
	6	1.32652 (1.3265)	1.29886	1.26095	1.24305	6.30
	7	2.36308 (2.3631)	2.27899	2.16275	2.00359	12.33
	8	2.37888 (2.3789)	2.30232	2.19865	2.04601	12.14
	9	2.49112 (2.4911)	2.49009	2.48909	2.48761	0.13
	10	3.66609 (3.6661)	3.53296	3.34164	3.09375	16.99
(2, 1)	1	0.151936 (0.15194)	0.150435	0.148281	0.144925	10.61
	2	0.638751 (0.63875)	0.638102	0.637136	0.635552	0.42
	3	1.07614 (1.0761)	1.06982	1.06017	1.04373	2.11
	4	1.24166 (1.2417)	1.24094	1.23959	1.22634	3.00
	5	1.34248 (1.3425)	1.31670	1.28178	1.24255	7.53
	6	1.63234 (1.6323)	1.60362	1.56411	1.50741	7.45
	7	2.38695 (2.3869)	2.31566	2.21391	2.06271	12.04
	8	2.48441 (2.4844)	2.46413	2.38392	2.26203	7.04
	9	2.56139 (2.5614)	2.50774	2.49233	2.48752	2.91
	10	3.67777 (3.6778)	3.54425	3.35376	3.10681	16.73

[a]Data in parentheses correspond to exact three-dimensional solution[15]; see Table 6 in Ref. 26.
[b]R.E. = relative error = $(\omega^*|_{R=0} - \omega^*|_{R=1.0})/\omega^*|_{R=0}$.

Similar to the bending problem, we investigate the free vibration of the rectangular laminate considered in Table 2 but with $a/h = 10$ only and for several different stacking sequence schemes. The lowest natural frequency parameter $\omega^* = \omega h\sqrt{(\rho/G_{LT})}$ $(m = n = 1)$ is shown in Table 4 where the formulations for cylindrical bending problem are directly employed to calculate the results for $b/h \to \infty$, which are also compared to other three-dimensional solutions.[27] It can be seen that the frequencies of the rectangular laminate converge rapidly to that of the laminate in cylindrical bending when b/a increases. In fact, the lowest natural frequency of the rectangular laminate of $b/a = 5$ has an error smaller than 1% when compared to that of the laminate in cylindrical bending. Thus, one can also treat the laminate as in a state of cylindrical bending when $b/a > 5$ for an initial dynamic analysis. In contrast to the bending problem, the frequency of the laminate in cylindrical bending is the lower limit, also because of the reduction of stiffness.

Conclusions

In this paper the static and dynamic behavior of simply supported cross-ply laminates featuring interlaminar bonding imperfections are investigated via the state-space approach. All formulations are directly based on the three-dimensional equations of an elastic orthotropic medium, without introducing any assumptions on deformations and stress fields like most plate theories. When perfect laminates are considered, the present formulations become exactly the same as that reported in literature. In fact, the treatment of boundary conditions at interfaces is rather straightforward. However, because of the lack of exact three-dimensional solutions of laminates with imperfect interfacial bonding the results presented in this paper are very valuable to other investigators for clarifying various simplified methods. In particular, the comparison made in this paper shows that although the plate theory developed in Cheng et al.[4] can always predict the behavior of perfect laminates well it will become inaccurate especially for thick laminates with interfacial bonding imperfections.

Although the methods presented by previous researchers[14,15] can be generalized to exactly analyze the laminates featuring interlaminar imperfections, they will become computationally uneconomic when the number of layers increases in the laminate. On the contrary, the state-space approach always leads to a linear algebraic eigenvalue problem with the same scale, just as illustrated in this paper.

Problem of cross-ply laminates with imperfect interfaces in cylindrical bending is also considered as a special case. Numerical results show that a rectangular laminate with one side five times longer than the other side can be treated as in a state of cylindrical bending for the purpose of simplified analysis.

Acknowledgment

The work was supported by the National Natural Science Foundation of China (No. 10002016).

References

[1]Whitney, J. M., *Structural Analysis of Laminated Anisotropic Plates*, Technomic, Lancaster, PA, 1987, pp. 1–15.

[2]Blandford, G. E., and Tauchert, T. R., "Thermoelastic Analysis of Layered Structures with Imperfect Layer Contact," *Computers and Structures*, Vol. 21, No. 6, 1985, pp. 1283–1291.

[3]Somers, M., Weller, T., and Abramovich, H., "Buckling and Postbuckling Behavior of Delaminated Sandwich Beams," *Composite Structures*, Vol. 21, No. 4, 1992, pp. 211–232.

[4]Cheng, Z. Q., Kennedy, D., and Williams, F. W., "Effect of Interfacial Imperfection on Buckling and Bending Behavior of Composite Laminates," *AIAA Journal*, Vol. 34, No. 12, 1996, pp. 2590–2595.

[5]Cheng, Z. Q., Jemah, A. K., and Williams, F. W., "Theory for Multilayered Anisotropic Plates with Weakened Interfaces," *Journal of Applied Mechanics*, Vol. 63, No. 4, 1996, pp. 1019–1026.

[6]Cheng, Z. Q., He, L. H., and Kitipornchai, S., "Influence of Imperfect Interfaces on Bending and Vibration of Laminated Composite Shells," *International Journal of Solids and Structures*, Vol. 37, No. 15, 2000, pp. 2127–2150.

[7]Aboudi, J., "Damage in Composites-Modelling of Imperfect Bonding," *Composites Science and Technology*, Vol. 28, No. 2, 1987, pp. 103–128.

[8]Hashin, Z., "The Spherical Inclusion with Imperfect Interface," *Journal of Applied Mechanics*, Vol. 58, No. 2, 1991, pp. 444–449.

[9]Di Sciuva, M., "Geometrically Nonlinear Theory of Multilayered Plates with Interlayer Slips," *AIAA Journal*, Vol. 35, No. 11, 1997, pp. 1753–1759.

[10]Icardi, U., "Free Vibration of Composite Beams Featuring Interlaminar Bonding Imperfections and Exposed to Thermomechanical Loading," *Composite Structures*, Vol. 46, No. 3, 1999, pp. 229–243.

[11]Icardi, U., Di Sciuva, M., and Librescu, L., "Dynamic Response of Adaptive Cross-Ply Cantilevers Featuring Interlaminar Bonding Imperfections," *AIAA Journal*, Vol. 38, No. 3, 2000, pp. 499–506.

[12]Librescu, L., and Schmidt, R., "A General Linear Theory of Laminated Composite Shells Featuring Interlaminar Bonding Imperfections," *International Journal of Solids and Structures*, Vol. 38, No. 19, 2001, pp. 3355–3375.

[13]Pagano, N. J., "Exact Solutions for Composite Laminates in Cylindrical Bending," *Journal of Composite Materials*, Vol. 3, No. 3, 1969, pp. 398–411.

[14]Pagano, N. J., and Hatfield, S. J., "Elastic Behavior of Multilayered Bidirectional Composites," *AIAA Journal*, Vol. 10, No. 7, 1972, pp. 931–933.

[15]Srinivas, S., Joga Rao, C. V., and Rao, A. K., "An Exact Analysis for Vibration of Simply-Supported Homogeneous and Laminated Thick Rectangular Plates," *Journal of Sound and Vibration*, Vol. 12, No. 2, 1970, pp. 187–199.

[16]Nosier, A., Kapania, R. K., and Reddy, J. N., "Free Vibration Analysis of Laminated Plates Using a Layerwise Theory," *AIAA Journal*, Vol. 31, No. 12, 1993, pp. 2335–2346.

[17]Jing, H. S., and Tzeng, K. G., "Elasticity Solution for Laminated Anisotropic Cylindrical Panels in Cylindrical Bending," *Composite Structures*, Vol. 30, No. 3, 1995, pp. 307–317.

[18]Kameswara Rao, N. S. V., and Das, Y. C., "A Mixed Method in Elasticity," *Journal of Applied Mechanics*, Vol. 44, No. 1, 1977, pp. 51–56.

[19]Fan, J. R., and Ye, J. Q., "An Exact Solution for the Statics and Dynamics of Laminated Thick Plates with Orthotropic Layer," *International Journal of Solids and Structures*, Vol. 26, No. 5/6, 1990, pp. 655–662.

[20]Ye, J. Q., and Soldatos, K. P., "Three-Dimensional Stress Analysis of Orthotropic and Cross-Ply Laminated Hollow Cylinders and Cylindrical Panels," *Computer Methods in Applied Mechanics and Engineering*, Vol. 117, No. 3–4, 1994, pp. 331–351.

[21]Chen, W. Q., and Ding, H. J., "A State-Space-Based Stress Analysis of a Multi-Layered Spherical Shell with Spherical Isotropy," *Journal of Applied Mechanics*, Vol. 68, No. 1, 2001, pp. 109–114.

[22]Chen, W. Q., and Ding, H. J., "Free Vibration of Multi-Layered Spherically Isotropic Hollow Sphere," *International Journal of Mechanical Sciences*, Vol. 43, No. 3, 2001, pp. 667–680.

[23]Chen, W. Q., Wang, L. Z., and Lu, Y., "Free Vibrations of Functionally Graded Piezoceramic Hollow Spheres with Radial Polarization," *Journal of Sound and Vibration*, Vol. 251, No. 1, 2002, pp. 103–114.

[24]Clegg, W. J., "The Fabrication and Failure of Laminar Ceramic Composites," *Acta Metallurgica et Materialia*, Vol. 40, No. 11, 1992, pp. 3085–3093.

[25]Spilker, R. L., Chou, S. C., and Orringer, O., "Alternate Hybrid-Stress Elements for Analysis of Multilayer Composite Plates," *Journal of Composite Materials*, Vol. 11, No. 1, 1977, pp. 51–70.

[26]Carrera, E., "A Study of Transverse Normal Stress Effect on Vibration of Multilayered Plates and Shells," *Journal of Sound and Vibration*, Vol. 225, No. 5, 1999, pp. 803–829.

[27]Messina, A., "Two Generalized Higher Order Theories in Free Vibration Studies of Multilayered Plates," *Journal of Sound and Vibration*, Vol. 242, No. 1, 2001, pp. 125–150.

A. Palazotto
Associate Editor